Supporting Information: Improvements and limitations of Mie λ-6 potential for prediction of saturated and compressed liquid viscosity

Richard A. Messerly

Thermodynamics Research Center, National Institute of Standards and Technology, Boulder, Colorado, 80305

Michelle C. Anderson

Thermodynamics Research Center, National Institute of Standards and Technology, Boulder, Colorado, 80305

S. Mostafa Razavi

Department of Chemical and Biomolecular Engineering, The University of Akron, Akron, Ohio, 44325-3906

J. Richard Elliott

Department of Chemical and Biomolecular Engineering, The University of Akron, Akron, Ohio, 44325-3906

SI.I. Systems simulated

Table SI.I enumerates the compounds, force fields, and viscosity types simulated in this study.

SI.II. Input files

We provide example input files for simulating 2,2,4-trimethylpentane at 245 K with the Potoff force field in GROMACS (see attached .gro, .top, and .mdp files). Additionally, all files necessary to generate the results from this study can be found at www.github.com/ramess101/IFPSC_10.

Email addresses: richard.messerly@nist.gov (Richard A. Messerly), michelle.anderson@nist.gov (Michelle C. Anderson), sr87@zips.uakron.edu (S. Mostafa Razavi), elliot1@uakron.edu (J. Richard Elliott)

Table SI.I: Compounds, force fields, and state points. "X": simulated, "O": not simulated, "S" simulated with "short" parameters, "L" simulated with "long" parameters.

	TraPPE (TraPPE-2)		Potoff (S/L)		AUA4		TAMie	
Compound	$\eta_{\text{liq}}^{\text{sat}}$	$\eta_{\text{liq}}^{\text{comp}}$	$\eta_{\text{liq}}^{\text{sat}}$	$\eta_{\text{liq}}^{\text{comp}}$	$\eta_{\text{liq}}^{\text{sat}}$	$\eta_{\text{liq}}^{\text{comp}}$	$\eta_{\text{liq}}^{\text{sat}}$	$\eta_{\text{liq}}^{\text{comp}}$
ethane	X (X)	X (X)	X	X	X	X	X	X
propane	X	X	X	X	O	O	X	X
n-butane	X	X	X	X	O	O	X	X
n-octane	X	X	X	X	O	O	X	X
n-dodecane	X	O	X	O	O	O	X	O
n-hexadecane	X	O	X	O	O	O	X	O
2-methylpropane	X	X	S	S	O	O	X	X
2-methylbutane	X	X	S	S	O	O	X	X
2,2-dimethylpropane	X	X	S	S	X	X	O	O
2,3-dimethylbutane	X	X	S	S	O	O	X	X
2-methylpentane	X	X	L	L	O	O	X	X
3-methylpentane	X	X	L	L	O	O	X	X
2,2,4-trimethylpentane	X	X	L	L	O	O	O	O

SI.III. Additional simulation details

Table SI.II lists the integrators, thermostats, and barostats used for each NPT or NVT stage.

SI.IV. Simulation time

For less viscous systems, i.e., saturation and low pressures, a 1 ns simulation is typically sufficient for the Green-Kubo integral to reach a plateau. However, even when there is an apparent plateau, systematic bias in η may still exist if the simulation is too short [1, 2]. For this reason, Figure SI.1 compares the Green-Kubo integral for simulations with

Table SI.II: Integrator, thermostat and barostat specifications.

	NPT Equil.	NPT Prod.	NVT Equil.	NVT Prod.
Integrator	Velocity Verlet	Leap frog	Velocity Verlet	Velocity Verl
Thermostat	Velocity rescale	Nosé-Hoover	Nosé-Hoover	Nosé-Hoove
Thermostat time-constant (ps)	1.0	1.0	1.0	1.0
Barostat	Berendsen	Parrinello-Rahman	N/A	N/A
Barostat time-constant (ps)	1.0	5.0	N/A	N/A
Barostat compressibility	4.5E-5	4.5E-5	N/A	N/A

0.5 ns, 1 ns, 2 ns, and 4 ns. We observe that the estimated viscosity obtained from a 1 ns trajectory is consistent with that from 2 ns and 4 ns simulations. Specifically, a plateau is observed at a similar value of η despite the large fluctuations at long times. We also note that 0.5 ns simulations are typically reliable but occasionally the plateau deviates considerably. For these reasons, the results presented in this study were obtained from 1 ns simulations.

For more viscous systems (greater than 0.02 Pa-s) a 1 ns simulation is too short to observe a plateau in the Green-Kubo integral. In these cases, we increase the simulation time to a value between 2 and 8 ns. Due to the increased computational cost of such simulations, we did not perform an exhaustive test with increasing simulation time. Instead, the choice of simulation time was determined primarily by the ability to detect a plateau region. Therefore, it is possible that even longer simulations are required for the most viscous systems.

Figure SI.2 depicts some of these highly viscous systems. Note that the total simulation time is twice the maximum time plotted. For example, an 8 ns run appears to be sufficient to detect a plateau for 2,2,4-trimethylpentane at 750 MPa, despite this system having a viscosity around 0.08 Pa-s. By contrast, a 1 ns run provides a reasonable plateau for the

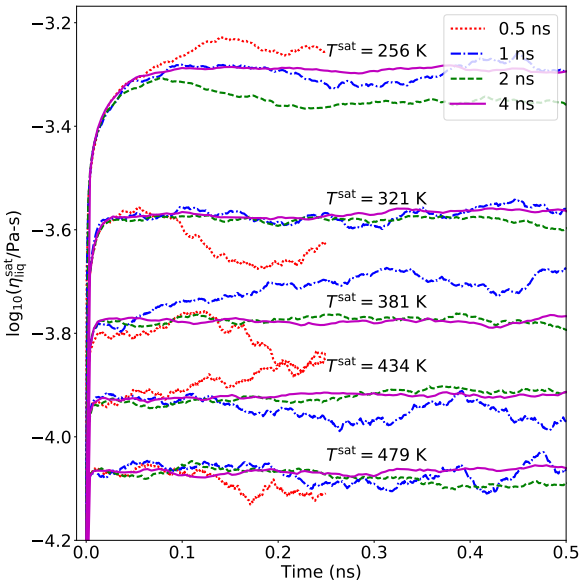

Figure SI.1: Simulation production time. Simulations were performed for *n*-octane using the TraPPE potential. Colors/line styles denote different simulation times (0.5 ns, 1 ns, 2 ns, and 4 ns).

other two systems with viscosities near 0.02 Pa-s.

SI.V. Validation Runs

To validate our methodology, we attempt to replicate viscosity estimates available on the NIST Standard Reference Simulation Website [3] for TraPPE-UA ethane as well as literature values for TraPPE-UA *n*-octane [4, 5]. Figures SI.3 and SI.4 compare the ethane and *n*-octane results, respectively.

The *n*-octane validation is somewhat more useful than the ethane validation for at least three reasons. First, *n*-octane includes angle and torsional contributions that are absent in ethane. Second, the literature provides values for both rigid and flexible bonds. Third, the *n*-octane results are at elevated pressures, which provides validation of our NPT ensemble results.

Figure SI.3 demonstrates that our results are consistent with the NIST Reference Simulation Data at higher densities, with some discrepancies at lower densities. Note that the NIST Standard Reference Simulation benchmark data were obtained with the NVE

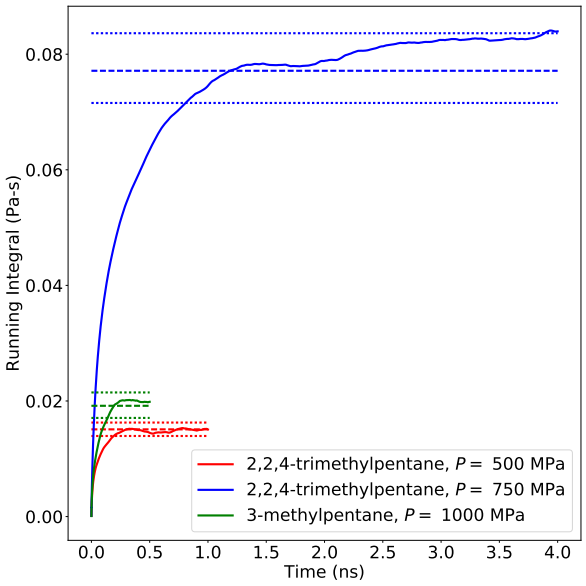

Figure SI.2: Green-Kubo integrals for the most viscous systems studied. Each compound was simulated with the Potoff potential. Solid lines are the average of N_{reps} replicates. Dashed lines are the estimated η value after fitting. Dotted lines represent the 95 % bootstrapped uncertainties.

ensemble, while our simulations were performed with the NVT ensemble at the average T reported on the NIST website. Also, the NIST simulations used 500 molecules, 250 ps production time, and a 0.5 fs time-step.

Figure SI.4 demonstrates that our results agree with the literature values for TraPPE *n*-octane at high pressures. Note that our flexible fond results utilize the same harmonic potential as Reference 4 ($k_{\text{b}}/k_{\text{B}} = 45.29$ K/pm^2, value actually reported in Reference 6). Thus, by comparing the circular points, there is an apparent positive bias between the Reference 4 values and those from this work. We note that Reference 4 utilizes NEMD simulations, where extrapolation to zero shear is necessary. From this result, we suggest that the extrapolation tends to over estimate the true viscosity. Furthermore, by comparing the fixed and flexible bond results we see a small shift towards higher viscosities for the harmonic potential. This is investigated further in Section SI.VI.

Recently, we became aware that Reference 5 utilizes a 1.0 nm cut-off, whereas we use a 1.4 nm cut-off. As demonstrated in Section 4 of the manuscript, the results for a 1.0 nm

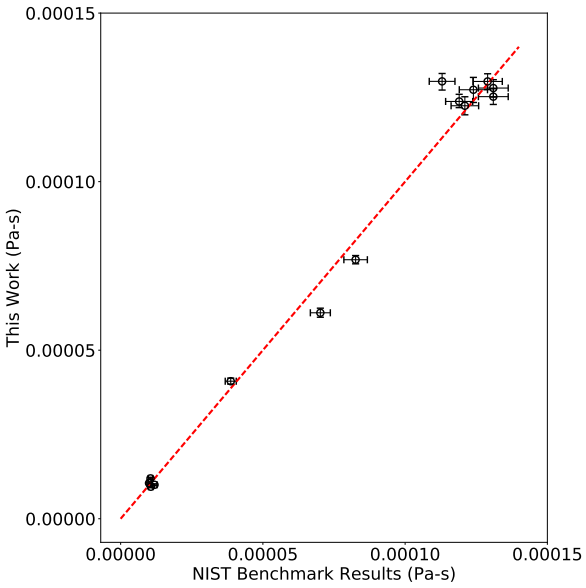

Figure SI.3: Comparison with NIST Standard Reference Simulation benchmark data [3]. Red line corresponds to $x = y$, i.e., exact agreement between this work and the NIST values. A constant uncertainty of 4 % is assumed for NIST values.

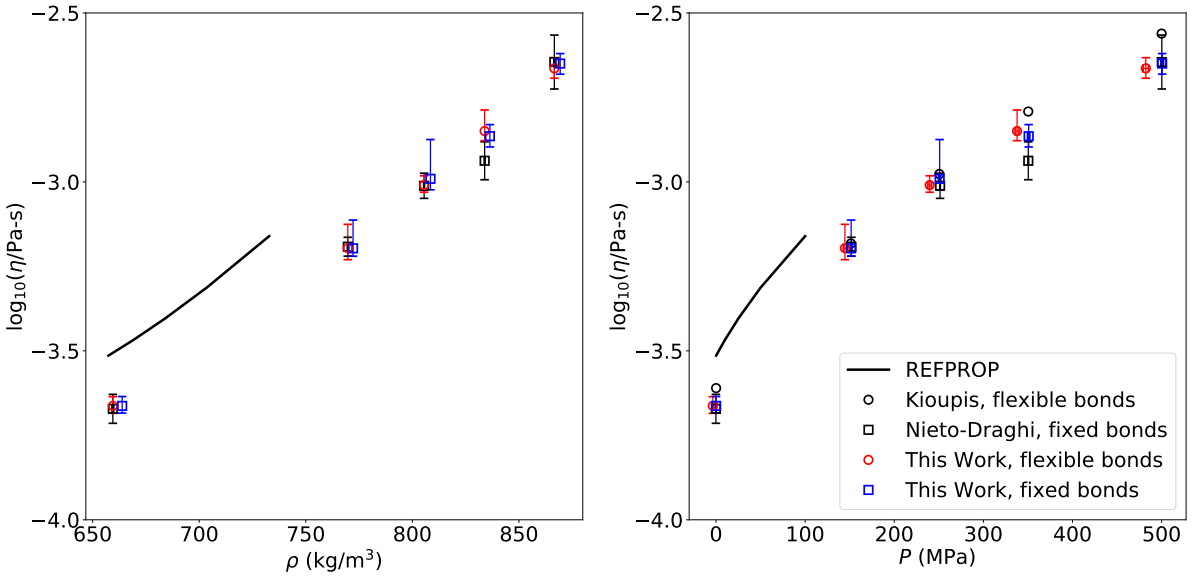

Figure SI.4: Comparison with Kioupis [4] and Nieto-Draghi [5]. Circle symbols were obtained with the same harmonic potential, while square symbols denote fixed bond-lengths.

and 1.4 nm cut-off can become significant for larger molecules. However, due to the good agreement between our values and those from Reference 5, the 1.0 nm cut-off appears to be sufficient for *n*-octane at elevated pressures. It is also worth noting that Reference 5 performed 10 to 20 ns simulations, while our simulation production time was only 1 ns.

Note that there appears to be a slight bias towards smaller box-sizes (higher ρ) for a given pressure when comparing the fixed bond-lengths from this work with the values of Reference 5. Also, small discrepancies exist between the state points reported in Reference 4 and Reference 5. This should not impact our validation, but it is somewhat curious. Also,

SI.VI. Fixed vs flexible bonds

Although static thermodynamic properties (e.g., $\rho_{\mathrm{liq}}^{\mathrm{sat}}$) are generally insensitive to the choice of fixed or flexible bonds, dynamic properties (e.g., η) can be much more sensitive. We perform simulations with flexible bonds to test how sensitive the results presented in this study are to the use of fixed bond-lengths. Specifically, we use the traditional harmonic bond potential:

$$u^{\mathrm{bond}} = \frac{k_{\mathrm{b}}}{2}\left(r - r_{\mathrm{eq}}\right)^2 \tag{1}$$

where u^{bond} is the bonded potential, k_{b} is the harmonic force constant, and r_{eq} is the equilibrium bond-length. We use an arbitrarily large value for the force constant, $k_{\mathrm{b}}/k_{\mathrm{B}} = 60.43$ K/pm^2, as this should result in a fairly stiff bonded potential, i.e., the bond-lengths should not vary significantly.

.

Figure SI.5 demonstrates that the difference between fixed and flexible bonds is negligible in certain cases. However, there is a small, but systematic, deviation towards higher viscosities for the stiff harmonic potential.

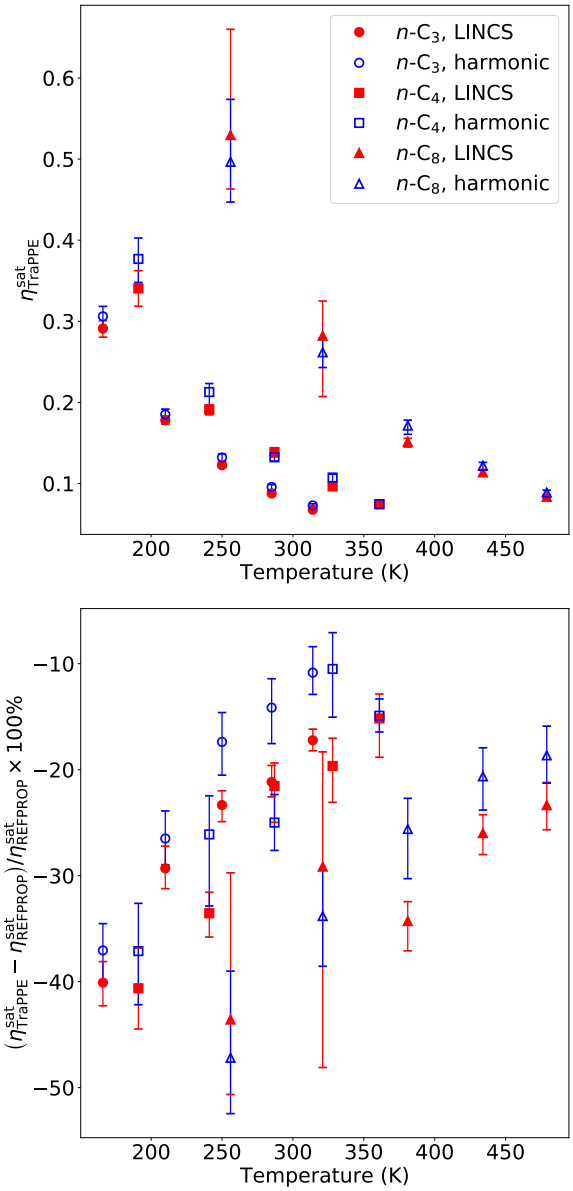

Figure SI.5: Fixed bond-lengths compared with an arbitrarily stiff harmonic bond potential. Simulations were performed using the TraPPE-UA force field. Colors/fill denote fixed or flexible bonds while symbol shape corresponds to different compounds.

SI.VII. Green-Kubo analysis

This section provides a detailed example of how we obtain estimates for η and the corresponding uncertainty. The results depicted in Figures SI.6 through SI.9 are for propane

with the Potoff model and $T^{\text{sat}} = 166$ K. Figure SI.6 depicts a typical autocorrelation function ("enecorr.xvg" file) obtained by executing the GROMACS "energy –vis" command. By default, GROMACS partitions the complete simulation into twelve evenly sized time blocks. Therefore, the autocorrelation function in Figure SI.6 is the average of twelve different time origins.

GROMACS then performs a simple two-point trapezoidal integration of neighboring points to obtain the Green-Kubo integral. The Green-Kubo integral with respect to time is output in the "visco.xvg" file. Figure SI.7 presents the Green-Kubo integral from forty replicate simulations. Although a single replicate is often quite noisy at long times, the average of these replicates converges smoothly (see Figure SI.7).

Figure SI.8 shows that the fluctuations, or standard deviation, increases with time but is adequately modeled with At^b. The line labeled "cut-off" in Figures SI.7 and SI.8 is the time at which $\sigma_\eta \approx 0.4 \times \eta^\infty$. Data beyond this time are excluded from the fit of the double-exponential function.

Bootstrap re-sampling provides an estimate of the uncertainty. Figure SI.9 shows that, typically, the bootstrapped distribution is quite normal. The lines labeled "bootstraps" in Figure SI.7 are the lower and upper 95 % confidence interval.

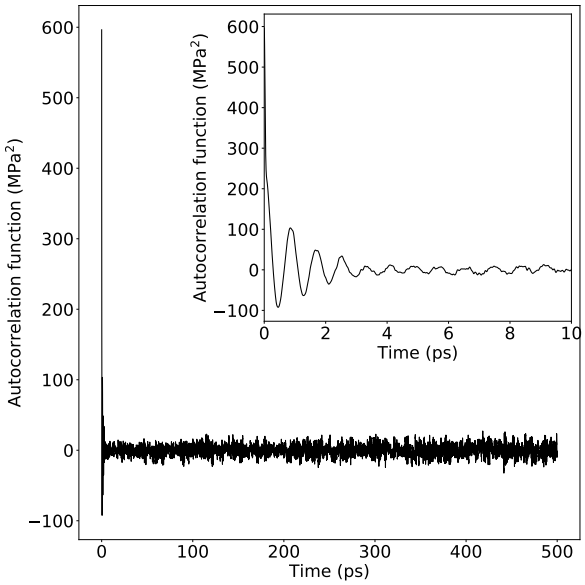

Figure SI.6: Autocorrelation function with respect to time.

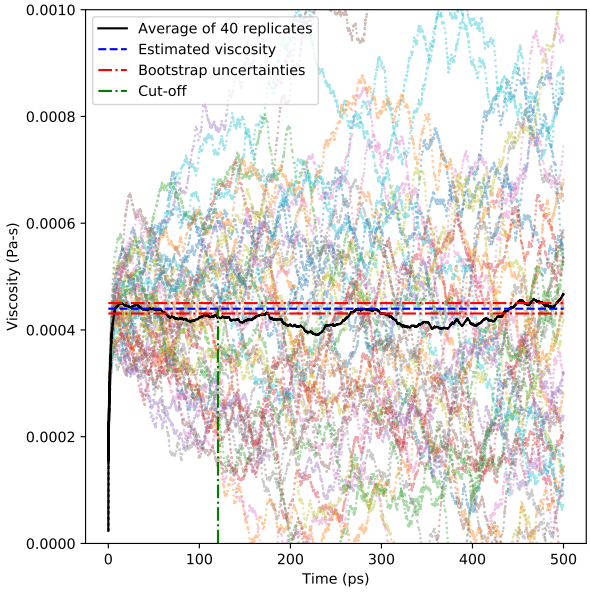

Figure SI.7: Replicate simulations, average, fit to average, bootstrap uncertainties, and cut-off.

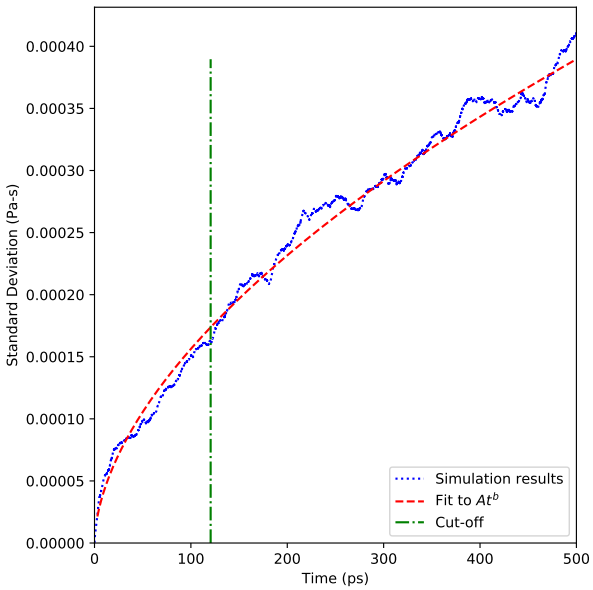

Figure SI.8: Standard deviation of replicate simulations with respect to time.

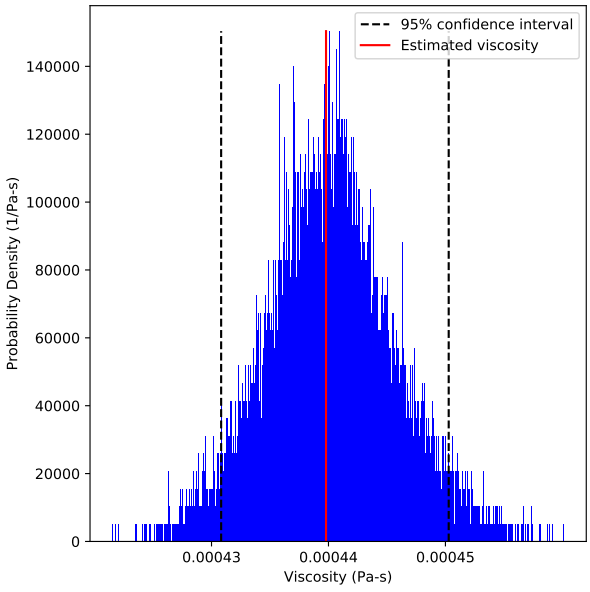

Figure SI.9: Bootstrap distribution of η.

SI.VIII. Tabulated values

Table SI.III: Saturated liquid viscosity values for ethane.

		Potoff	TAMie	TraPPE	AUA4	TraPPE-2
T^{sat} [K]	$\rho_{\mathrm{liq}}^{\mathrm{sat}}$ [kg/m^3]	$\eta_{\mathrm{liq}}^{\mathrm{sat}}$ [Pa-s]	$\eta_{\mathrm{liq}}^{\mathrm{sat}}$ [Pa-s]	$\eta_{\mathrm{liq}}^{\mathrm{sat}}$ [Pa-s]	$\eta_{\mathrm{liq}}^{\mathrm{sat}}$ [Pa-s]	$\eta_{\mathrm{liq}}^{\mathrm{sat}}$ [Pa-s]
137	600.04	$0.516_{0.024}$	$0.389_{0.013}$	$0.313_{0.014}$	$0.321_{0.011}$	$0.2981_{8.5\mathrm{E}-3}$
174	557.16	$0.2338_{4.8\mathrm{E}-3}$	$0.2046_{4.0\mathrm{E}-3}$	$0.1714_{3.7\mathrm{E}-3}$	$0.1741_{4.1\mathrm{E}-3}$	$0.1773_{3.3\mathrm{E}-3}$
207	514.33	$0.1499_{3.3\mathrm{E}-3}$	$0.1360_{3.0\mathrm{E}-3}$	$0.1123_{2.5\mathrm{E}-3}$	$0.1185_{3.6\mathrm{E}-3}$	$0.1204_{2.1\mathrm{E}-3}$
236	471.45	$0.0991_{2.4\mathrm{E}-3}$	$0.0976_{2.1\mathrm{E}-3}$	$0.0844_{1.8\mathrm{E}-3}$	$0.0837_{2.2\mathrm{E}-3}$	$0.0876_{1.2\mathrm{E}-3}$
260	428.60	$0.0732_{1.3\mathrm{E}-3}$	$0.0709_{1.3\mathrm{E}-3}$	$0.0623_{1.1\mathrm{E}-3}$	$0.0629_{1.9\mathrm{E}-3}$	$0.0661_{1.3\mathrm{E}-3}$

Table SI.IV: Saturated liquid viscosity values for propane.

		Potoff	TAMie	TraPPE
T^{sat} [K]	$\rho_{\mathrm{liq}}^{\mathrm{sat}}$ [kg/m^3]	$\eta_{\mathrm{liq}}^{\mathrm{sat}}$ [Pa-s]	$\eta_{\mathrm{liq}}^{\mathrm{sat}}$ [Pa-s]	$\eta_{\mathrm{liq}}^{\mathrm{sat}}$ [Pa-s]
86	732.21	$10.7_{1.5}$	$5.31_{0.40}$	$2.47_{0.16}$
90	728.03	$8.34_{0.96}$	$4.42_{0.22}$	$2.01_{0.12}$
100	717.71	$3.56_{0.22}$	$2.53_{0.18}$	$1.243_{0.049}$
110	707.53	$2.17_{0.12}$	$1.500_{0.060}$	$0.898_{0.039}$
130	687.26	$1.003_{0.033}$	$0.844_{0.026}$	$0.517_{0.013}$
166	651.14	$0.439_{0.011}$	$0.389_{0.013}$	$0.2967_{8.3\mathrm{E}-3}$
210	604.63	$0.2482_{9.4\mathrm{E}-3}$	$0.2361_{9.5\mathrm{E}-3}$	$0.1800_{4.0\mathrm{E}-3}$
250	558.12	$0.1513_{4.9\mathrm{E}-3}$	$0.1498_{5.3\mathrm{E}-3}$	$0.1234_{3.1\mathrm{E}-3}$
285	511.61	$0.1040_{3.2\mathrm{E}-3}$	$0.1055_{3.8\mathrm{E}-3}$	$0.0874_{1.5\mathrm{E}-3}$
314	465.10	$0.0761_{1.9\mathrm{E}-3}$	$0.0797_{2.6\mathrm{E}-3}$	$0.0676_{1.2\mathrm{E}-3}$

Table SI.V: Saturated liquid viscosity values for *n*-butane.

		Potoff	TAMie	TraPPE
T^{sat} [K]	$\rho_{\mathrm{liq}}^{\mathrm{sat}}$ [kg/m^3]	$\eta_{\mathrm{liq}}^{\mathrm{sat}}$ [Pa-s]	$\eta_{\mathrm{liq}}^{\mathrm{sat}}$ [Pa-s]	$\eta_{\mathrm{liq}}^{\mathrm{sat}}$ [Pa-s]
191	341.27	$0.545_{0.056}$	$0.604_{0.030}$	$0.336_{0.029}$
241	316.89	$0.279_{0.016}$	$0.2664_{6.2\mathrm{E}-3}$	$0.1900_{4.3\mathrm{E}-3}$
287	292.52	$0.1691_{3.7\mathrm{E}-3}$	$0.1640_{3.7\mathrm{E}-3}$	$0.1327_{2.7\mathrm{E}-3}$
328	268.14	$0.1146_{2.5\mathrm{E}-3}$	$0.1168_{1.8\mathrm{E}-3}$	$0.0928_{2.0\mathrm{E}-3}$
361	243.76	$0.0858_{1.6\mathrm{E}-3}$	$0.0849_{2.1\mathrm{E}-3}$	$0.0726_{1.2\mathrm{E}-3}$

Table SI.VI: Saturated liquid viscosity values for *n*-octane.

		Potoff	TAMie	TraPPE
T^{sat} [K]	$\rho_{\mathrm{liq}}^{\mathrm{sat}}$ [kg/m^3]	$\eta_{\mathrm{liq}}^{\mathrm{sat}}$ [Pa-s]	$\eta_{\mathrm{liq}}^{\mathrm{sat}}$ [Pa-s]	$\eta_{\mathrm{liq}}^{\mathrm{sat}}$ [Pa-s]
256	732.07	$0.830_{0.041}$	$0.870_{0.029}$	$0.504_{0.019}$
321	679.78	$0.373_{0.011}$	$0.373_{0.010}$	$0.2675_{7.0\mathrm{E}-3}$
381	627.49	$0.2231_{0.010}$	$0.2378_{5.9\mathrm{E}-3}$	$0.1689_{4.9\mathrm{E}-3}$
434	575.20	$0.1385_{5.9\mathrm{E}-3}$	$0.1416_{3.5\mathrm{E}-3}$	$0.1161_{2.8\mathrm{E}-3}$
479	522.91	$0.1053_{4.7\mathrm{E}-3}$	$0.1024_{7.4\mathrm{E}-3}$	$0.0851_{2.4\mathrm{E}-3}$

Table SI.VII: Saturated liquid viscosity values for *n*-dodecane.

		Potoff	TAMie	TraPPE
T^{sat} [K]	$\rho_{\mathrm{liq}}^{\mathrm{sat}}$ [kg/m^3]	$\eta_{\mathrm{liq}}^{\mathrm{sat}}$ [Pa-s]	$\eta_{\mathrm{liq}}^{\mathrm{sat}}$ [Pa-s]	$\eta_{\mathrm{liq}}^{\mathrm{sat}}$ [Pa-s]
296	747.27	$1.056_{0.065}$	$1.009_{0.048}$	$0.691_{0.049}$
362	698.31	$0.487_{0.024}$	$0.487_{0.014}$	$0.349_{0.014}$
427	647.90	$0.2768_{8.1\mathrm{E}-3}$	$0.2868_{8.7\mathrm{E}-3}$	$0.2180_{7.0\mathrm{E}-3}$
493	590.68	$0.1799_{5.5\mathrm{E}-3}$	$0.1780_{7.0\mathrm{E}-3}$	$0.1442_{5.0\mathrm{E}-3}$
559	520.47	$0.1066_{2.8\mathrm{E}-3}$	$0.1114_{4.3\mathrm{E}-3}$	$0.0937_{2.1\mathrm{E}-3}$

Table SI.VIII: Saturated liquid viscosity values for *n*-hexadecane.

		Potoff	TAMie	TraPPE
T^{sat} [K]	$\rho_{\mathrm{liq}}^{\mathrm{sat}}$ [kg/m^3]	$\eta_{\mathrm{liq}}^{\mathrm{sat}}$ [Pa-s]	$\eta_{\mathrm{liq}}^{\mathrm{sat}}$ [Pa-s]	$\eta_{\mathrm{liq}}^{\mathrm{sat}}$ [Pa-s]
325	751.26	$1.225_{0.092}$	$1.217_{0.094}$	$0.794_{0.047}$
397	700.84	$0.572_{0.027}$	$0.568_{0.023}$	$0.439_{0.017}$
469	648.85	$0.364_{0.025}$	$0.329_{0.017}$	$0.264_{0.010}$
541	592.22	$0.1956_{6.4\mathrm{E}-3}$	$0.1917_{6.9\mathrm{E}-3}$	$0.1752_{6.1\mathrm{E}-3}$
613	524.45	$0.1296_{3.5\mathrm{E}-3}$	$0.1249_{4.0\mathrm{E}-3}$	$0.1114_{4.7\mathrm{E}-3}$

Table SI.IX: Saturated liquid viscosity values for *n*-docosane.

		Potoff	TAMie	TraPPE
T^{sat} [K]	$\rho_{\mathrm{liq}}^{\mathrm{sat}}$ [kg/m^3]	$\eta_{\mathrm{liq}}^{\mathrm{sat}}$ [Pa-s]	$\eta_{\mathrm{liq}}^{\mathrm{sat}}$ [Pa-s]	$\eta_{\mathrm{liq}}^{\mathrm{sat}}$ [Pa-s]
435	700.85	$0.626_{0.028}$	$0.677_{0.046}$	$0.529_{0.026}$
514	647.14	$0.384_{0.016}$	$0.381_{0.014}$	$0.341_{0.016}$
594	588.70	$0.2422_{8.6\mathrm{E}-3}$	$0.246_{0.010}$	$0.1901_{7.1\mathrm{E}-3}$
673	521.32	$0.1368_{4.5\mathrm{E}-3}$	$0.1540_{5.5\mathrm{E}-3}$	$0.1267_{4.3\mathrm{E}-3}$

Table SI.X: Saturated liquid viscosity values for 2-methylpropane.

		Potoff	TAMie	TraPPE
T^{sat} [K]	$\rho_{\mathrm{liq}}^{\mathrm{sat}}$ [kg/m^3]	$\eta_{\mathrm{liq}}^{\mathrm{sat}}$ [Pa-s]	$\eta_{\mathrm{liq}}^{\mathrm{sat}}$ [Pa-s]	$\eta_{\mathrm{liq}}^{\mathrm{sat}}$ [Pa-s]
184	673.41	$0.546_{0.017}$	$0.3630_{9.7\mathrm{E}-3}$	$0.347_{0.019}$
232	625.31	$0.2706_{6.6\mathrm{E}-3}$	$0.2189_{5.2\mathrm{E}-3}$	$0.2016_{4.5\mathrm{E}-3}$
276	577.21	$0.1612_{3.5\mathrm{E}-3}$	$0.1403_{3.1\mathrm{E}-3}$	$0.1316_{2.3\mathrm{E}-3}$
315	529.11	$0.1175_{2.1\mathrm{E}-3}$	$0.1028_{2.9\mathrm{E}-3}$	$0.0941_{1.8\mathrm{E}-3}$
347	481.01	$0.0845_{1.8\mathrm{E}-3}$	$0.0761_{1.4\mathrm{E}-3}$	$0.0737_{1.6\mathrm{E}-3}$

Table SI.XI: Saturated liquid viscosity values for 2-methylbutane.

		Potoff	TAMie	TraPPE
T^{sat} [K]	$\rho_{\mathrm{liq}}^{\mathrm{sat}}$ [kg/m^3]	$\eta_{\mathrm{liq}}^{\mathrm{sat}}$ [Pa-s]	$\eta_{\mathrm{liq}}^{\mathrm{sat}}$ [Pa-s]	$\eta_{\mathrm{liq}}^{\mathrm{sat}}$ [Pa-s]
207	700.98	$0.648_{0.019}$	$0.475_{0.014}$	$0.396_{0.021}$
261	650.91	$0.3056_{8.8\mathrm{E}-3}$	$0.2647_{9.3\mathrm{E}-3}$	$0.2134_{8.4\mathrm{E}-3}$
312	600.84	$0.1815_{4.3\mathrm{E}-3}$	$0.1700_{5.0\mathrm{E}-3}$	$0.1452_{6.7\mathrm{E}-3}$
356	550.77	$0.1190_{2.6\mathrm{E}-3}$	$0.1201_{3.7\mathrm{E}-3}$	$0.1022_{3.9\mathrm{E}-3}$
392	500.70	$0.0897_{1.5\mathrm{E}-3}$	$0.0883_{2.5\mathrm{E}-3}$	$0.0771_{3.4\mathrm{E}-3}$

Table SI.XII: Saturated liquid viscosity values for 2-methylpentane.

		Potoff	TAMie	TraPPE
T^{sat} [K]	$\rho_{\mathrm{liq}}^{\mathrm{sat}}$ [kg/m^3]	$\eta_{\mathrm{liq}}^{\mathrm{sat}}$ [Pa-s]	$\eta_{\mathrm{liq}}^{\mathrm{sat}}$ [Pa-s]	$\eta_{\mathrm{liq}}^{\mathrm{sat}}$ [Pa-s]
224	713.87	$0.572_{0.016}$	$0.501_{0.019}$	$0.330_{0.014}$
282	662.88	$0.2848_{9.6\mathrm{E}-3}$	$0.2551_{7.6\mathrm{E}-3}$	$0.2069_{5.9\mathrm{E}-3}$
337	611.89	$0.1763_{4.3\mathrm{E}-3}$	$0.1690_{4.5\mathrm{E}-3}$	$0.1371_{3.1\mathrm{E}-3}$
384	560.90	$0.1219_{3.0\mathrm{E}-3}$	$0.1196_{2.6\mathrm{E}-3}$	$0.0998_{2.1\mathrm{E}-3}$
423	509.91	$0.101_{0.010}$	$0.0868_{2.0\mathrm{E}-3}$	$0.0748_{1.4\mathrm{E}-3}$

Table SI.XIII: Saturated liquid viscosity values for 3-methylpentane.

		Potoff	TAMie	TraPPE
T^{sat} [K]	$\rho_{\mathrm{liq}}^{\mathrm{sat}}$ [kg/m^3]	$\eta_{\mathrm{liq}}^{\mathrm{sat}}$ [Pa-s]	$\eta_{\mathrm{liq}}^{\mathrm{sat}}$ [Pa-s]	$\eta_{\mathrm{liq}}^{\mathrm{sat}}$ [Pa-s]
227	723.49	$0.587_{0.024}$	$0.545_{0.019}$	$0.392_{0.012}$
278	678.27	$0.341_{0.016}$	$0.3090_{8.6\mathrm{E}-3}$	$0.2423_{7.3\mathrm{E}-3}$
328	632.19	$0.2060_{5.6\mathrm{E}-3}$	$0.1913_{5.0\mathrm{E}-3}$	$0.1700_{9.3\mathrm{E}-3}$
379	579.98	$0.1325_{2.6\mathrm{E}-3}$	$0.1282_{2.7\mathrm{E}-3}$	$0.1131_{2.5\mathrm{E}-3}$
430	515.73	$0.0882_{1.6\mathrm{E}-3}$	$0.0895_{1.9\mathrm{E}-3}$	$0.0778_{1.4\mathrm{E}-3}$

Table SI.XIV: Saturated liquid viscosity values for 2,2-dimethylpropane.

		Potoff	AUA4	TraPPE
T^{sat} [K]	$\rho_{\mathrm{liq}}^{\mathrm{sat}}$ [kg/m^3]	$\eta_{\mathrm{liq}}^{\mathrm{sat}}$ [Pa-s]	$\eta_{\mathrm{liq}}^{\mathrm{sat}}$ [Pa-s]	$\eta_{\mathrm{liq}}^{\mathrm{sat}}$ [Pa-s]
257	627.44	$0.325_{0.024}$	$0.1694_{3.6\mathrm{E}-3}$	$0.2172_{5.5\mathrm{E}-3}$
300	582.62	$0.1780_{4.8\mathrm{E}-3}$	$0.1212_{2.3\mathrm{E}-3}$	$0.1404_{3.4\mathrm{E}-3}$
337	537.80	$0.1219_{1.9\mathrm{E}-3}$	$0.0919_{3.4\mathrm{E}-3}$	$0.1006_{1.9\mathrm{E}-3}$
368	492.99	$0.0889_{1.6\mathrm{E}-3}$	$0.0746_{4.1\mathrm{E}-3}$	$0.0782_{1.4\mathrm{E}-3}$
393	448.17	$0.0667_{1.2\mathrm{E}-3}$	$0.0572_{1.2\mathrm{E}-3}$	$0.0591_{1.4\mathrm{E}-3}$

Table SI.XV: Saturated liquid viscosity values for 2,3-dimethylbutane.

		Potoff	TAMie	TraPPE
T^{sat} [K]	$\rho_{\mathrm{liq}}^{\mathrm{sat}}$ [kg/m^3]	$\eta_{\mathrm{liq}}^{\mathrm{sat}}$ [Pa-s]	$\eta_{\mathrm{liq}}^{\mathrm{sat}}$ [Pa-s]	$\eta_{\mathrm{liq}}^{\mathrm{sat}}$ [Pa-s]
225	719.43	$0.898_{0.035}$	$0.579_{0.019}$	$0.478_{0.013}$
275	677.37	$0.410_{0.013}$	$0.332_{0.015}$	$0.2756_{7.1\mathrm{E}-3}$
325	632.13	$0.270_{0.011}$	$0.218_{0.010}$	$0.1938_{5.6\mathrm{E}-3}$
375	580.70	$0.1621_{6.3\mathrm{E}-3}$	$0.1466_{6.3\mathrm{E}-3}$	$0.1324_{2.4\mathrm{E}-3}$
425	517.24	$0.1076_{4.4\mathrm{E}-3}$	$0.0926_{2.3\mathrm{E}-3}$	$0.0869_{1.6\mathrm{E}-3}$

Table SI.XVI: Saturated liquid viscosity values for 2,2,4-trimethylpentane.

		Potoff	TraPPE
T^{sat} [K]	$\rho_{\mathrm{liq}}^{\mathrm{sat}}$ [kg/m^3]	$\eta_{\mathrm{liq}}^{\mathrm{sat}}$ [Pa-s]	$\eta_{\mathrm{liq}}^{\mathrm{sat}}$ [Pa-s]
245	730.93	$0.807_{0.046}$	$0.450_{0.023}$
309	678.72	$0.390_{0.014}$	$0.255_{0.013}$
369	626.51	$0.245_{0.013}$	$0.1654_{7.8\mathrm{E}-3}$
421	574.30	$0.1488_{3.2\mathrm{E}-3}$	$0.1199_{6.8\mathrm{E}-3}$
464	522.09	$0.1035_{1.6\mathrm{E}-3}$	$0.1009_{5.8\mathrm{E}-3}$

Table SI.XVII: Compressed liquid viscosity values for propane.

		Potoff		TAMie		TraPPE	
T [K]	$\rho_{\text{liq}}^{\text{comp}}$ [kg/m^3]	P [MPa]	$\eta_{\text{liq}}^{\text{comp}}$ [Pa-s]	P [MPa]	$\eta_{\text{liq}}^{\text{comp}}$ [Pa-s]	P [MPa]	$\eta_{\text{liq}}^{\text{comp}}$ [Pa-s]
293	500.28	$-0.11_{0.39}$	$0.0987_{2.4\text{E}-3}$	$0.54_{0.35}$	$0.0966_{4.3\text{E}-3}$	$0.71_{0.45}$	$0.0831_{3.0\text{E}-3}$
293	559.78	$40.48_{0.45}$	$0.1595_{4.2\text{E}-3}$	$41.14_{0.53}$	$0.183_{0.024}$	$32.51_{0.56}$	$0.1211_{2.2\text{E}-3}$
293	629.11	$156.03_{0.63}$	$0.318_{0.015}$	$154.23_{0.58}$	$0.316_{0.023}$	$117.77_{0.74}$	$0.2185_{7.9\text{E}-3}$
293	654.75	$228.00_{0.96}$	$0.3950_{8.0\text{E}-3}$	$223.73_{0.81}$	$0.364_{0.013}$	$168.77_{0.79}$	$0.2720_{8.3\text{E}-3}$
293	681.80	$328.1_{1.8}$	$0.579_{0.020}$	$318.8_{1.4}$	$0.525_{0.027}$	$237.7_{1.1}$	$0.3346_{8.8\text{E}-3}$
293	710.37	$466.6_{1.4}$	$0.840_{0.022}$	$449.4_{1.0}$	$0.676_{0.027}$	$330.85_{0.98}$	$0.420_{0.010}$
293	740.56	$658.7_{1.2}$	$1.291_{0.072}$	$627.74_{0.72}$	$1.22_{0.11}$	$455.94_{0.86}$	$0.618_{0.024}$
293	772.48	$925.08_{0.72}$	$2.370_{0.096}$	$871.66_{0.69}$	$1.611_{0.076}$	$624.13_{0.72}$	$0.842_{0.031}$
293	806.26	$1295.21_{0.81}$	$5.23_{0.28}$	$1205.57_{0.63}$	$2.68_{0.12}$	$849.83_{0.91}$	$1.360_{0.070}$

Table SI.XVIII: Compressed liquid viscosity values for *n*-butane.

		Potoff		TAMie		TraPPE	
T [K]	$\rho_{\text{liq}}^{\text{comp}}$ [kg/m^3]	P [MPa]	$\eta_{\text{liq}}^{\text{comp}}$ [Pa-s]	P [MPa]	$\eta_{\text{liq}}^{\text{comp}}$ [Pa-s]	P [MPa]	$\eta_{\text{liq}}^{\text{comp}}$ [Pa-s]
293	578.76	$1.51_{0.43}$	$0.1568_{4.0\text{E}-3}$	$4.92_{0.44}$	$0.1611_{8.6e-3}$	$-0.05_{0.49}$	$0.1339_{7.4\text{E}-3}$
293	618.15	$38.98_{0.53}$	$0.2242_{4.7\text{E}-3}$	$43.98_{0.51}$	$0.2362_{5.2e-3}$	$28.12_{0.54}$	$0.1754_{7.7\text{E}-3}$
293	661.20	$110.51_{0.62}$	$0.3633_{9.7\text{E}-3}$	$116.62_{0.46}$	$0.377_{0.017}$	$80.01_{0.55}$	$0.249_{0.010}$
293	708.33	$242.33_{0.73}$	$0.695_{0.034}$	$247.68_{0.62}$	$0.628_{0.019}$	$171.74_{0.76}$	$0.351_{0.015}$
293	760.06	$481.6_{1.1}$	$1.483_{0.061}$	$479.67_{0.98}$	$1.317_{0.061}$	$330.31_{0.79}$	$0.643_{0.036}$

Table SI.XIX: Compressed liquid viscosity values for *n*-octane.

		Potoff		TAMie		TraPPE	
T [K]	$\rho_{\text{liq}}^{\text{comp}}$ [kg/m^3]	P [MPa]	$\eta_{\text{liq}}^{\text{comp}}$ [Pa-s]	P [MPa]	$\eta_{\text{liq}}^{\text{comp}}$ [Pa-s]	P [MPa]	$\eta_{\text{liq}}^{\text{comp}}$ [Pa-s]
293	702.44	$1.15_{0.65}$	$0.508_{0.034}$	$13.64_{0.63}$	$0.505_{0.020}$	$-6.37_{0.47}$	$0.324_{0.014}$
293	764.16	$123.47_{0.83}$	$1.435_{0.076}$	$142.97_{0.98}$	$1.148_{0.070}$	$77.88_{0.59}$	$0.657_{0.024}$
293	832.65	$405.1_{7.6}$	$5.93_{0.64}$	$426.7_{2.8}$	$6.02_{0.41}$	$260.9_{1.1}$	$1.790_{0.084}$
293	894.90	$870.6_{1.4}$	$68.0_{4.9}$	$881.09_{0.81}$	$36.2_{2.9}$	$548.29_{0.99}$	$5.29_{0.84}$
293	921.79	–	–	–	–	$719.6_{1.1}$	$11.7_{1.1}$

Table SI.XX: Compressed liquid viscosity values for 2-methylpropane.

	Potoff			TAMie			
T [K]	$\rho_{\text{liq}}^{\text{comp}}$ [kg/m^3]	P [MPa]	$\eta_{\text{liq}}^{\text{comp}}$ [Pa-s]	$\rho_{\text{liq}}^{\text{comp}}$ [kg/m^3]	P [MPa]	$\eta_{\text{liq}}^{\text{comp}}$ [Pa-s]	$\rho_{\text{liq}}^{\text{comp}}$ [k
293	$558.6_{1.2}$	$-0.03_{0.91}$	$0.1501_{6.3\text{E}-3}$	$1.72_{0.23}$	$0.0758_{9.5\text{E}-3}$	2.71 E-$3_{3.4\text{E}-4}$	559.
293	$626.45_{0.53}$	$69.9_{1.3}$	$0.287_{0.016}$	$636.45_{0.93}$	$62.7_{5.6}$	$0.2338_{8.9\text{E}-3}$	640.0
293	$752.08_{0.25}$	$500.2_{2.3}$	$1.676_{0.066}$	$770.48_{0.39}$	$491.1_{2.4}$	$1.077_{0.034}$	786.1
293	$787.35_{0.18}$	$750.2_{2.6}$	$3.53_{0.17}$	$806.17_{0.25}$	$723.3_{2.5}$	$1.87_{0.20}$	827.9
293	$813.97_{0.19}$	$1001.1_{2.4}$	$6.90_{0.42}$	$833.55_{0.14}$	$952.0_{2.2}$	$3.25_{0.12}$	860.0

Table SI.XXI: Compressed liquid viscosity values for 2-methylbutane.

	Potoff			TAMie			
T [K]	$\rho_{\text{liq}}^{\text{comp}}$ [kg/m^3]	P [MPa]	$\eta_{\text{liq}}^{\text{comp}}$ [Pa-s]	$\rho_{\text{liq}}^{\text{comp}}$ [kg/m^3]	P [MPa]	$\eta_{\text{liq}}^{\text{comp}}$ [Pa-s]	$\rho_{\text{liq}}^{\text{comp}}$ [kg/m
293	$617.83_{0.58}$	$-0.17_{0.75}$	$0.2233_{9.6\text{E}-3}$	$622.94_{0.59}$	$-0.21_{0.71}$	$0.1968_{4.0\text{E}-3}$	$622.35_{0.83}$
293	$741.30_{0.21}$	$249.9_{1.2}$	$0.925_{0.039}$	$751.79_{0.19}$	$250.0_{1.2}$	$0.816_{0.028}$	$767.87_{0.23}$
293	$792.67_{0.19}$	$500.1_{1.4}$	$2.32_{0.10}$	$805.79_{0.17}$	$499.8_{1.5}$	$1.90_{0.11}$	$828.04_{0.17}$
293	$827.36_{0.21}$	$749.9_{2.3}$	$5.73_{0.50}$	$842.47_{0.20}$	$748.8_{2.2}$	$4.09_{0.22}$	$869.12_{0.18}$
293	$854.00_{0.20}$	$1000_{2.9}$	$12.4_{1.1}$	$869.29_{0.38}$	$982.7_{4.0}$	$8.54_{0.84}$	$900.99_{0.14}$

Table SI.XXII: Compressed liquid viscosity values for 3-methylpentane.

	Potoff			TAMie			
T [K]	$\rho_{\text{liq}}^{\text{comp}}$ [kg/m^3]	P [MPa]	$\eta_{\text{liq}}^{\text{comp}}$ [Pa-s]	$\rho_{\text{liq}}^{\text{comp}}$ [kg/m^3]	P [MPa]	$\eta_{\text{liq}}^{\text{comp}}$ [Pa-s]	$\rho_{\text{liq}}^{\text{comp}}$ [kg/m
293	$647.42_{0.68}$	$-0.18_{0.86}$	$0.2312_{5.7\text{E}-3}$	$660.41_{0.46}$	$-0.08_{0.60}$	$0.2528_{6.8\text{E}-3}$	$667.88_{0.50}$
293	$768.20_{0.22}$	$250.0_{1.3}$	$1.079_{0.049}$	$778.92_{0.24}$	$250.1_{1.0}$	$1.099_{0.048}$	$800.52_{0.25}$
293	$819.29_{0.20}$	$500.3_{1.8}$	$2.61_{0.13}$	$831.42_{0.18}$	$500.5_{1.6}$	$2.78_{0.19}$	$858.95_{0.18}$
293	$854.04_{0.22}$	$750.2_{2.4}$	$8.71_{0.97}$	$867.56_{0.22}$	$750.5_{2.3}$	$6.53_{0.55}$	$899.32_{0.19}$
293	$880.81_{0.31}$	$1000_{4.3}$	$19.2_{2.3}$	$895.60_{0.30}$	$999.9_{4.0}$	$18.0_{2.1}$	$930.76_{0.20}$

Table SI.XXIII: Compressed liquid viscosity values for 2,2,4-trimethylpentane.

	Potoff			TraPPE		
T [K]	$\rho_{\text{liq}}^{\text{comp}}$ [kg/m^3]	P [MPa]	$\eta_{\text{liq}}^{\text{comp}}$ [Pa-s]	$\rho_{\text{liq}}^{\text{comp}}$ [kg/m^3]	P [MPa]	$\eta_{\text{liq}}^{\text{comp}}$ [Pa-s]
293	$691.60_{0.64}$	$-1.88_{0.98}$	$0.432_{0.013}$	$704.21_{0.84}$	$-1.7_{1.0}$	$0.3299_{8.5\text{E}-3}$
293	$788.98_{0.33}$	$207.1_{1.6}$	$2.24_{0.11}$	$817.59_{0.33}$	$206.9_{1.3}$	$1.455_{0.069}$
293	$848.66_{0.34}$	$499.9_{2.8}$	$15.1_{1.2}$	$887.40_{0.28}$	$499.7_{1.8}$	$4.91_{0.20}$
293	$881.93_{0.59}$	$750.5_{6.0}$	$77.2_{6.5}$	$926.81_{0.29}$	$750.5_{2.4}$	$15.02_{0.78}$
293	–	–	–	$957.44_{0.44}$	$1000.5_{4.3}$	$49.5_{5.4}$

References for Supporting Information

References

[1] Edward J. Maginn, Richard A. Messerly, Daniel J. Carlson, Daniel R. Roe, and J. Richard Elliott. Best practices for computing transport properties 1. Self-diffusivity and viscosity from equilibrium molecular dynamics v1. *Living Journal of Computational Molecular Science*, Pending publication, 2018.

[2] Yong Zhang, Akihito Otani, and Edward J. Maginn. Reliable viscosity calculation from equilibrium molecular dynamics simulations: A time decomposition method. *Journal of Chemical Theory and Computation*, 11(8):3537–3546, 2015.

[3] Vince K. Shen, Daniel W. Siderius, William P. Krekelberg, and Harold W. Hatch. NIST standard reference simulation website, NIST standard reference database number 173. *National Institute of Standards and Technology*, Gaithersburg MD, 20899.

[4] Loukas I. Kioupis and Edward J. Maginn. Impact of molecular architecture on the high-pressure rheology of hydrocarbon fluids. *The Journal of Physical Chemistry B*, 104(32):7774–7783, 2000.

[5] Carlos Nieto-Draghi, Philippe Ungerer, and Bernard Rousseau. Optimization of the anisotropic united atoms intermolecular potential for *n*-alkanes: Improvement of transport properties. *The Journal of Chemical Physics*, 125(4):044517, 2006.

[6] Loukas I. Kioupis and Edward J. Maginn. Molecular simulation of poly-α-olefin synthetic lubricants: impact of molecular architecture on performance properties. *The Journal of Physical Chemistry B*, 103(49):10781–10790, 1999.